ELSEVIER

Polymer 41 (2000) 2121–2126

polymer

Scanning probe microscopy of pine and birch kraft pulp fibres

J. Simola[a], P. Malkavaara[b], R. Alén[b], J. Peltonen[a,*]

[a]*Department of Physical Chemistry, Åbo Akademi University, Porthansgatan 3-5, FIN-20500 Turku, Finland*
[b]*Laboratory of Applied Chemistry, University of Jyväskylä, P.O. Box 35, FIN-40351 Jyväskylä, Finland*

Received 1 January 1999; received in revised form 12 April 1999; accepted 25 May 1999

Abstract

Fibres of the conventional pine and birch kraft pulps were characterized by scanning probe microscopy (SPM). The surface characteristics of these pulps taken at the early stages of pulping were compared with those from later stages of pulping (with or without subsequent oxygen/alkali delignification). It was observed that during delignification a granular surface structure was replaced by a fibrillar surface containing various disruptions. The granular and fibrillar regions were particularly well resolved by using phase imaging in tapping mode of SPM. It was concluded that the granular structure corresponded to surface lignin since the decrease in the relative amount of the granular phase correlated well to a decreasing kappa value of pulps. The surface concentration of lignin, e.g. at the end of pulping was much higher than the bulk lignin concentration. Eventually individual microfibrils (estimated diameter ranging from 0.01 to 0.03 μm) were observed for both pulps in the cases where delignification was almost completed.

Keywords: SPM; Phase imaging; Kraft pulp fibres

1. Introduction

In a tapping mode scanning probe microscope (TM-SPM) the cantilever is excited into resonance oscillation with a piezoelectric driver and the oscillation amplitude is used as a feedback signal to track the surface topography. The phase imaging technique is a special imaging mode of TM-SPM. The phase of oscillation of the cantilever changes when the probe encounters surface regions of different adhesion, stiffness or viscoelastic composition. Generally, close to zero or slightly negative phase shifts refer to a stickier (e.g. more hydrophilic) or softer surface, whereas a positive phase shift indicates a relatively harder or stiffer surface. Phase imaging has recently been applied on different materials including detailed studies on the factors affecting the phase contrast, i.e. the absolute (free) amplitude and damping ratio of tapping, the role of adhesion as well as the nature of the viscoelastic tip–sample interaction [1–10]. Closely related to our study, Chernoff [1] has published phase images of wood pulp fibres revealing a fine structure and material contrast which were barely seen in the topographical data. Two different phase regions were observed: (i) light amorphous material, suggested to be hydrophobic lignin, and (ii) microfibrillar dark material, hydrophilic cellulose.

The main chemical constituents of wood are macromolecules [11,12]. Native cellulose is a linear (ca. 5 μm) homopolysaccharide consisting of β-(1 → 4)-linked D-glucopyranose moieties aligned in bundles, so-called microfibrils of 100–500 cellulose chains. Hemicelluloses are slightly branched heteropolysaccharides consisting of different monosaccharide units such as D-glucose, D-mannose, D-galactose, D-xylose and L-arabinose. Lignin is a polymer of phenylpropane units linked to each other in various types of ether and carbon-to-carbon linkages. The main goal of pulping is to break down most of these linkages, which results in a simultaneous depolymerization and dissolution of lignin.

The pulp fibre research with SPM has mostly focused on model celluloses at nanometer scale [13–17] and studies on the properties of the isolated polymers [18,19]. Especially, detection of differences between hemicelluloses and cellulose has been difficult at the mesoscopic level because of the heterogeneity of the surface. Individual microfibrils are linked by hemicelluloses and lignin and it is supposed that the actual morphology and chemical behavior of lignin and related substances under pulping conditions are strongly influenced by surrounding organic and inorganic matrices. In intact wood polar cellulose fibres affect lignin morphology [18].

In spite of the relevance to the pulp and paper industry it has proven difficult to relate chemical and morphological structure of wood, although the main chemical constituents of wood, i.e. cellulose, hemicelluloses and lignin are well characterized. Because the exact location of each component

* Corresponding author. Tel.: +358-2-215-4252; fax: +358-2-215-4706.

0032-3861/00/$ - see front matter
PII: S0032-3861(99)00379-1

Table 1
Some characteristics of the pulp samples

Sample	Cooking time (min)	SCAN[a] kappa number	Bulk lignin amount (%)	Yield (% on wood)	SCAN[b] viscosity (cm^3/g)	Arithmetic Length of fibre (mm)
Birch 1	10	27.4	4.11	45.59	1101	0.96
Birch 2	200	15.1	2.30	43.95	1047	0.81
Pine 1	10	72.8	10.92	56.58	1012	1.80
Pine 2	220[c]	3.2	0.48	35.74[d]	366[d]	1.49[d]

[a] SCAN-C 1:77.
[b] SCAN-CM 15:88.
[c] Oxygen delignification.
[d] Values before oxygen/alkali delignification.

in fibre ultrastructure has not been possible to point out, it has been difficult to measure the interactions between the chemical components of an individual fibre wall. The aim of this work was to localize these main components in hardwood and softwood kraft pulp fibres and especially to compare the surface concentration of lignin with its bulk concentration. A reliable and convenient method for recognizing hemicelluloses from cellulose and, on the other hand, both of these carbohydrates from lignin would be a useful tool in monitoring, for example, chemical changes in the fibre surface during different delignification processes. In this study, we report an early micrometer scale SPM characterization of wood fibres at the beginning and at the end of delignification and relate these results to images of the chemically pure kraft lignin. Special attention was paid on tuning the measuring parameters in phase imaging.

2. Experimental

2.1. Materials

Pulp samples with varying cooking times were obtained by laboratory-scale conventional kraft cooking [20] of pine (*Pinus sylvestris*) and birch (*Betula pendula*) chips (cooking temperature 170°C, which was reached from 80°C by heating with a rate of 1°C/min). Selected pine pulp samples were further subjected to oxygen/alkali delignification treatment at 90°C (reaction time: 60 min, O_2: pressure 5 bar). Some characteristics of these samples are summarized in Table 1. Prior to imaging the pulp samples were pretreated with distilled water and dried on sample stubs covered by double-sided adhesive tape.

The lignin sample was isolated and purified from the black liquor obtained from the pine cook having 100 min cooking time at the maximum temperature. The kappa number of the corresponding pulp was 13.7 and the cooking yield 40.4% of the initial wood. The kappa number test is a standardized indirect method for determining the lignin content of pulps (SCAN Norm C 1:77). The lignin was precipitated by lowering the pH value of black liquor to 2.0 with 2 M HCl, separated by centrifugation, washed thoroughly with acidified water and dried under an air atmosphere at room temperature [21]. For the measurements, the brown powder obtained was slightly pressed on double-sided tape on the sample stub.

2.2. SPM measurements

The SPM images were recorded with a Nanoscope IIIa microscope (Digital Instruments Inc., Santa Barbara, CA), equipped with the extender electronics module enabling phase imaging in the tapping mode. All samples were imaged in tapping mode, capturing dual height and phase images. Silicon cantilevers with a resonance frequency of 250–300 kHz were used. When engaging the surface the resonance of the cantilever shifted towards smaller frequencies.

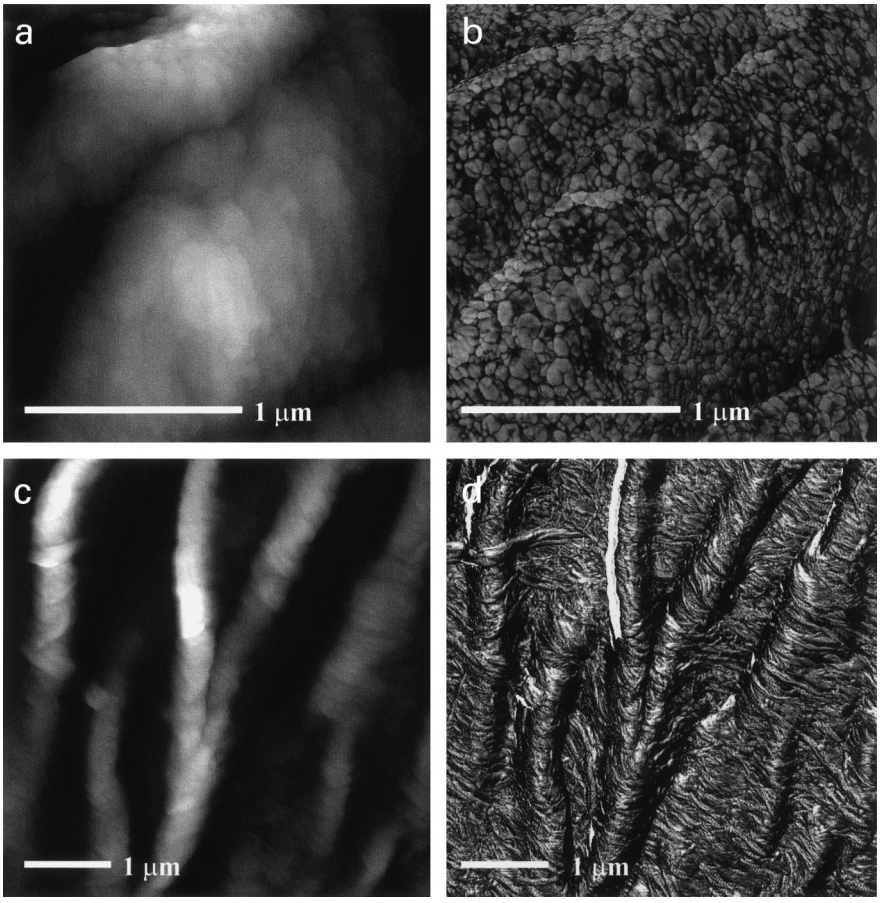

Fig. 1. SPM topographic (a,c) and phase (b,d) images of 10 min cooked (a,b; image size 2 μm) and 220 min cooked and oxygen delignified (c,d; image size 5 μm) pine kraft pulp samples. The *Z*-scales for images a–d are 300 nm, 30°, 600 nm and 100°.

Therefore, before engaging, the drive frequency was set about 250 Hz below resonance. The trace and retrace signals were set identical before image capture. Unless otherwise mentioned the set-point amplitude/free amplitude ratio (A_{sp}/A_0) was between 0.4 and 0.8 and scan rates from 0.7 to 1.7 Hz were used. The free amplitude varied between 50 and 70 nm. All images (512 × 512 pixels) were measured in air. Scan size varied between 500 nm and 10 μm. Filtering was not used during scanning. The measuring unit was placed on a massive stone table acting as a vibration isolator to eliminate external noise.

3. Results and discussion

3.1. Images of the pulp and lignin samples

The images shown in Fig. 1 represent typical surface structures of the pine pulp samples both at the beginning of pulping and after an almost complete lignin removal by pulping and oxygen delignification. These results clearly reveal the resolution difference between the height and phase images. The topographs (Fig. 1(a) and (c)) resolved the main bundles of microfibrils and their rough surface structure. The phase images resolved, in addition, the granular (Fig. 1(b)) and fibrillar (Fig. 1(d)) fine structures of the bundles of microfibrils. The diameter of the grains was in the order of 50–100 nm and height between 10 and 25 nm. Fibrils in Fig. 1(d) were about 50 nm wide. The given dimensions were directly measured from the images without considering the tip–sample convolution effect.

It is evident from Fig. 1(b) and (d) that the granular surface structure of the 10 min cooked pine pulp sample had disappeared as a result of 220 min cooking and oxygen/alkali delignification and that the fibrillar structure had appeared instead. According to the kappa values (Table 1) the total amount of lignin decreased from 10.9 to 0.5%, respectively. This supports the image interpretation that the observed grains correspond to the surface lignin. However, the possibility that part of the grains correspond to hemicelluloses or even extractives cannot be excluded. In the completely delignified sample the initial bundles of microfibrils seemed to have dispersed into smaller units being vertically aligned in the image. Part of the linear structure in Fig. 1(d) could be recognized to be individual microfibrils. However, part of the fine structure being oriented perpendicular to the microfibril bundles clearly lacked the characteristics of continuous microfibrils; in fact in this case

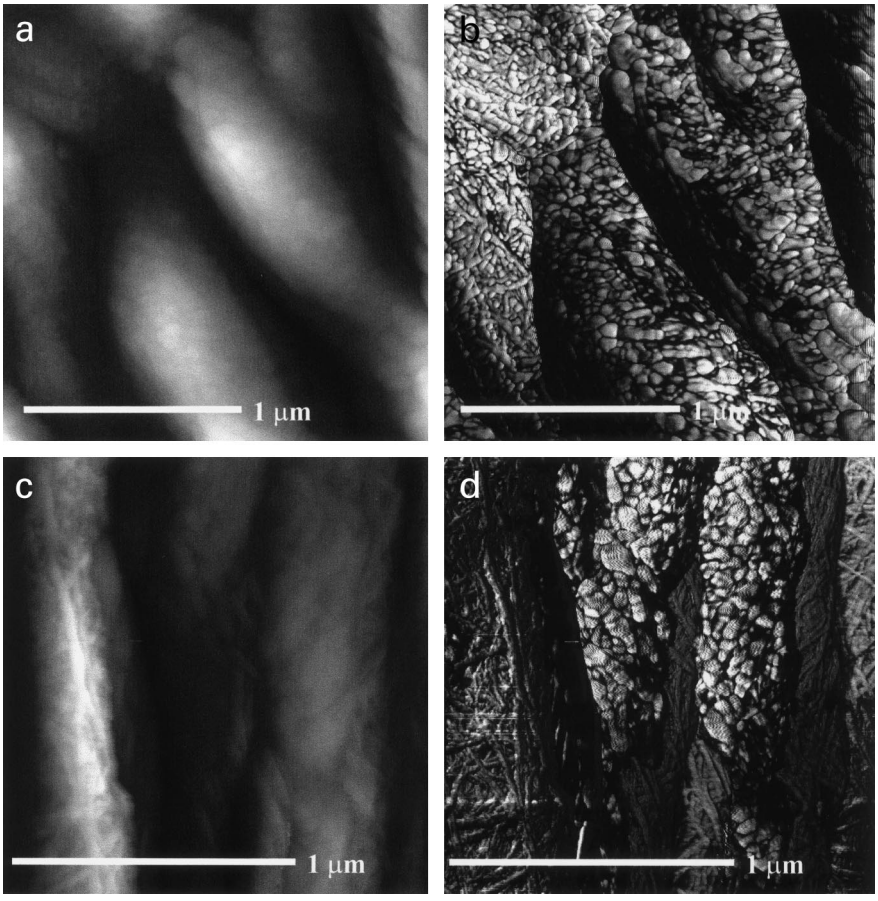

Fig. 2. SPM topographic (a,c) and phase (b,d) images of 10 min cooked (a,b; image size 2 μm) and 220 min cooked (c,d; image size 1.5 μm) birch kraft pulp samples. The *Z*-scales for images a–d are 300 nm, 30°, 500 nm and 50°.

the fine structure referred to a degraded surface. Thus, it is concluded that the degradation of fibres is a risk factor if the oxygen delignification is continued beyond the removal of the majority of surface lignin [22]. It should be noted that the narrow white sector in the upper part of image 1d most probably represents an imaging artifact. The trace–retrace phase signals differed strongly from each other within this narrow sector, whereas elsewhere on the surface the signals were identical and qualifications for stable imaging were good.

The height image of Fig. 2(a) for the birch pulp sample after 10 min cooking shows fibrils with a horizontal width in the order of 0.5–0.7 μm. From the respective phase image of Fig. 2(b) the mean diameter of the grains was measured to be about 35–120 nm which is close to that observed for the pine pulp samples. If also the convolution effect would be taken into consideration the estimated diameter would be slightly smaller (radius of curvature *R* of the used cantilever tips was 10–20 nm according to the manufacturer) [13]. The three-dimensional model for lignin proposed by Jurasek [23] suggests that a lignin molecule of MW ca. 55 000 (DP = 300) would have a diameter of some 20 nm. This correlates to the smallest spherical structures observed in this investigation. However, it should be kept in mind that the molecular weight of lignosulfonates may vary for various samples between 400 and 150 000 g/mol (and for pine kraft lignins between 1800 and 51 000 g/mol) [24].

The birch pulp samples resembled the pine pulp samples in that the granular surface structure decreased and the fibrillar surface content increased as a function of delignification, the structural details being again best resolved in the phase images (Fig. 2). The diameter of the fibrils was in the range of 0.04–0.125 μm which corresponds to a bundle of microfibrils, individual microfibrils supposed to be ca. 20 nm in diameter. The birch pulp sample after 200 min cooking was, however, not purely fibrillar, which is especially well demonstrated in the phase image of Fig. 2(d). Some grains are still visible on the surface. The same size distribution and form of the grains in Fig. 2 as compared with those seen for the pine pulp sample (Fig. 1) suggests that they both represent the lignin being initially bound to the fibres and not, e.g. lignin or extractives reprecipitated on the surface of the fibres. It is worth noting that the total amount of lignin for the samples of 2(a)–(d) was 4.1 and 2.3% (Table 1) whereas the images indicate an almost 100% lignin coverage at the beginning and still ca. 10–40% lignin coverage at the end of pulping. The high surface lignin content is in agreement with the results reported by Laine

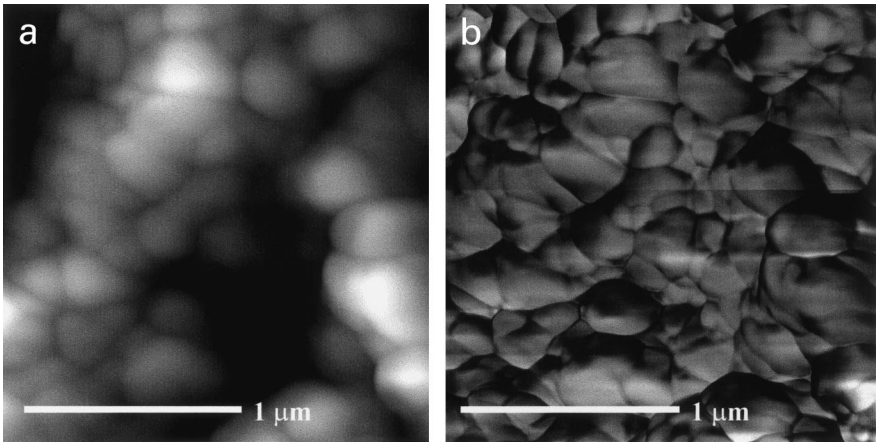

Fig. 3. Surface of the kraft pine lignin sample. (a) 2 μm AFM height (height scale = 400 nm) and (b) phase image (height scale = 40°).

et al. [25,26] concerning an ESCA study: during cooking the surface lignin content decreased linearly with a decreasing amount of total lignin (total lignin content >3%), but the surface lignin content was about five times higher than the average content of lignin in the fibres. They also concluded that there might be both reprecipitated lignin and some remnants of lignin-rich material such as middle lamella on the surface of fibres.

Finally, the structure of the isolated and reprecipitated lignin (average molecular mass 2092 g/mol) was studied in order to obtain further proof for the presented image interpretation. As seen in Fig. 3, the structure of the pure lignin is granular as expected but the grain size (diameter 0.2–0.5 μm) is much larger than that of the surface lignin of the pulp samples shown in Figs. 1 and 2. This indicates that the structure of the bound and dissolved lignin is markedly different and dependent on a number of factors, including the separation technique applied.

3.2. Theoretical considerations of phase imaging

The factors giving rise to the image contrast in phase imaging deserve to be discussed further. The spring constant k of a freely oscillating cantilever will change by σ to a new effective spring constant k_e when the cantilever starts interacting with the sample [2]:

$$k_e = k + \sigma = k + \sigma_s + \sigma_{cl}. \quad (1)$$

σ has been split into two terms; σ_s describing the tip–sample interaction and σ_{cl} corresponding to the tip–contamination layer interaction [2]. Furthermore, the contamination layer is dominated by the water content of the surface. In 'light-tapping' imaging slight damping of oscillation is used ($A_{sp}/A_0 \approx 0.8$) meaning that relatively weak tip–sample interaction takes place. Then, if a contrast appears in the phase image it is most probably dominated by σ_{cl}, whereas σ_s gives only a weak contribution [2,6]. The contrast of the phase image in Fig. 1(b), as an example of light tapping ($A_{sp}/A_0 = 0.75$), looks rather weak, indicating that the surface is quite homogeneous. Thus, σ_{cl} can be concluded to be constant over the whole surface and the only factor contributing to the phase contrast is actually the grain boundaries. The phase image of Fig. 2(d), also representing light tapping ($A_{sp}/A_0 = 0.72$), does show a fair contrast between the light grains and darker fibres, which most probably refers to an amphiphilic contrast through locally varying σ_{cl} (hydrophobic lignin vs. hydrophilic cellulose) rather than to a stiffness contrast. Chernoff [1] has reported on a similar kind of contrast for wood fibres although direct comparisons are not possible since the exact tapping conditions are not given in that article.

In moderate tapping the tip–sample interaction becomes stronger with an increased damping of oscillation. Then, as recently described [2,6], σ_s becomes gradually the dominating term causing the shift of k_e. With this assumption, $\sigma_s \gg \sigma_{cl}$, the Hertz model can be applied. σ_s is hence proportional to the sample stiffness S which again is proportional to the tip–sample contact area A and the effective modulus E^*:

$$S \propto A^{1/2} E^*. \quad (2)$$

Fig. 1(c) and (d) has been taken under 'moderate tapping' ($A_{sp}/A_0 \approx 0.6$) conditions. The height image appears slightly distorted, whereas the phase image resolves a very detailed surface structure down to individual microfibrils. Obviously, increasing the contrast in the phase image by increasing the imaging force through increased damping results in a decreased resolution of the topograph. No clear areas of specific phase shift appear on the surface. As a matter of fact, the dark contrast visible in the valleys between the fibres may refer to local differences in adhesion force and possibly high local water content at the surface. This indicates that in these valleys, despite the moderate tapping, the attractive forces (giving rise to negative phase shift) are dominating the tip–sample interaction rather than sample indentation, which induces a repulsive force and a positive phase shift.

It is worth commenting that 'hard tapping' was difficult to apply for the studied pulp samples. In other words, the smaller the used A_{sp}/A_0 ratio was (i.e. ca. 0.4 or less) the more technical difficulties were noticed. Another typical problem with these samples was the difficulty to capture phase images larger than 5 μm without observing artifacts (distorted images, lost contact in some part of image, non-identical trace–retrace scope etc.) and disturbances. These facts indicate that the samples were quite rough on large scale and relatively soft which may give rise to a phase contrast that is dominated by increasing contact area contribution with increasing tapping force.

4. Conclusions

The surface structure of the pine and birch pulp samples was studied with TM-SPM. The clear resolution difference between the height and phase mode imaging was observed and the 'light-tapping' and 'moderate-tapping' phase imaging were concluded to be effective methods to resolve surface fine structure of wood fibres. The images of the pulp samples taken at the early stage of the kraft pulping showed a granular structure, whereas the images of pulp samples from later stages of cooking (with or without a subsequent oxygen/alkali delignification) were mostly fibrillar. The surface concentration of the granular structure was observed to be much higher than the bulk lignin concentration of the samples. The size of the smallest spherical grains coincided fairly with the theoretical literature value of a lignin molecule. The phase images with best resolution could resolve individual microfibrils with a diameter of 0.01–0.03 μm. This preliminary study will be expanded in the forthcoming study including more samples from the different stages of delignification. These data will be useful when determining the stages where an accelerated desorption of lignin takes place or where the risk of fibre damage becomes meaningful. In addition, the phase imaging parameters need more careful screening and control, e.g. tuning of the tapping amplitude and carrying out the measurements under controlled environmental conditions.

Acknowledgements

This work was financially supported by the Technology Development Centre (TEKES) of Finland.

References

[1] Chernoff DA. Pol Prepr 1996;37:599.
[2] Whangbo MH, Bar G, Brandsch R. Appl Phys A 1998;66:S1267.
[3] Bar G, Thomann Y, Brandsch R, Cantow HJ, Whangbo MH. Langmuir 1997;13:3807.
[4] Sarid D, Hunt JP, Workman RK, Yao X, Peterson CA. Appl Phys A 1998;66:S283.
[5] García R, Tamayo J, Calleja M, García F. Appl Phys A 1998;66: S309.
[6] Whangbo MH, Magonov SN, Bengel H. Probe Microscopy 1997;1:23.
[7] Tamayo J, García R. Langmuir 1996;12:4430.
[8] Leclère Ph, Lazzaroni R, Brédas JL, Yu JM, Dubois Ph, Jérôme R. Langmuir 1996;12:4317.
[9] Brandsch R, Bar G, Whangbo MH. Langmuir 1997;13:6349.
[10] Spatz JP, Sheiko S, Möller M, Winkler RG, Reineker P, Marti O. Langmuir 1997;13:4699.
[11] Fengel D, Wegener G. Wood-chemistry, ultrastructure, reactions. Berlin, Germany: Walter de Gruyter, 1989. p. 613.
[12] Sjöström E. Wood chemistry-fundamentals and applications, 2nd edn. San Diego, USA: Academic Press, 1992. p. 293.
[13] Hanley SJ, Griasson J, Revol JF, Gray DG. Polymer 1992;33: 4639.
[14] Hanley SJ, Gray DG. Holzforschung 1994;48:29.
[15] Kuutti L, Peltonen J, Pere J, Teleman O. J Microscopy 1995;178:1.
[16] Baker AA, Helbert W, Sugiyama J, Miles MJ. J Struct Biol 1997;119:129.
[17] Holmberg M, Berg J, Stemme S, Ödberg L, Rasmusson J, Claesson P. J Colloid Interface Sci 1997;186:369.
[18] Shevchenko SM, Bailey GW, Shane Yu Y, Akim LG. Tappi J 1996;79:227.
[19] Pereira DED. Claudio-da-Silva Jr. E. Proceedings of the 8th International Symposium on Wood and Pulping Chemistry, Helsinki, 1, 1995, p. 467.
[20] Mimms A, Kocurek MJ, Pyatte J, Wright E. Kraft pulping; a compilation of notes, 2nd edn. Atlanta, GA, USA: TAPPI Press, 1993. 181.
[21] Alén R, Hartus T. Cellul Chem Technol 1988;22:613.
[22] McDonough TJ. Oxygen delignification. In: Dence CW, Reeves DW, editors. Pulping bleaching -principles and practice. Atlanta: Tappi Press, 1996. p. 217 Section IV, Chapter 1.
[23] Jurasek L. J Pulp Paper Sci 1995;21(8):J274.
[24] Goring DAI. Polymer properties of lignin and lignin derivatives. In: Sarkanen KV, Ludwig CH, editors. Lignins; occurrence, formation, structure and reactions. New York: Wiley-Interscience, 1971. p. 695.
[25] Laine J, Stenius P, Carlsson G, Ström G. Cellulose 1 1994;2:145.
[26] Laine J, Stenius P, Buchert J. Proc. 48th Appita Annual General Conference, Parkville, 1994, 109.